

4K4DGen: Panoramic 4D Generation at 4K Resolution

Renjie Li¹, Panwang Pan^{1*}, Bangbang Yang¹, Dejia Xu², Shijie Zhou³, Xuanyang Zhang¹,
Zeming Li¹, Achuta Kadambi³, Zhangyang Wang², Zhiwen Fan²

¹Pico ²UT Austin ³UCLA

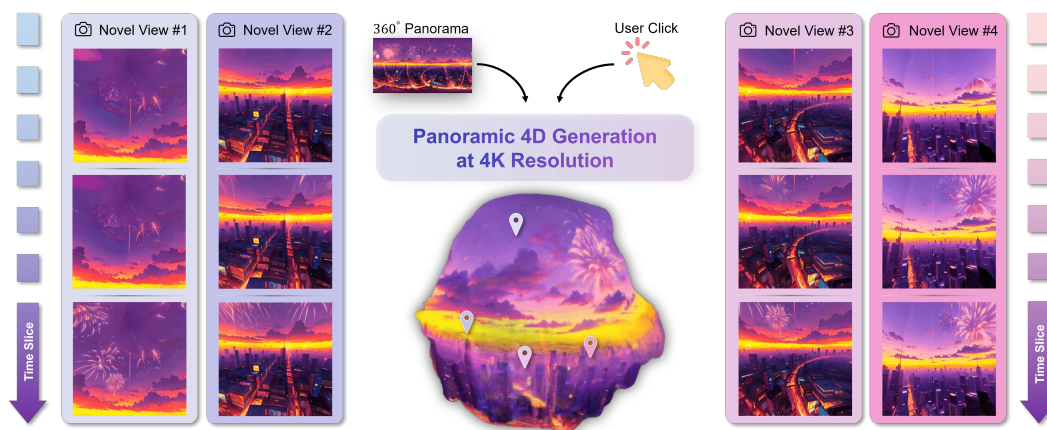


Figure 1: **4K4DGen** accepts a static panoramic image at a resolution of 4096×2048 . Upon user interaction through designated clicks, it animates specific regions and converts them into 4D point-based representations. This functionality enables real-time rendering of novel views and dynamic timestamps, thereby enhancing immersive virtual exploration.

Abstract

The blooming of virtual reality and augmented reality (VR/AR) technologies has driven an increasing demand for the creation of high-quality, immersive, and dynamic environments. However, existing generative techniques either focus solely on dynamic objects or perform outpainting from a single perspective image, failing to meet the needs of VR/AR applications. In this work, we tackle the challenging task of elevating a single panorama to an immersive 4D experience. For the first time, we demonstrate the capability to generate omnidirectional dynamic scenes with 360-degree views at 4K resolution, thereby providing an immersive user experience. Our method introduces a pipeline that facilitates natural scene animations and optimizes a set of 4D Gaussians using efficient splatting techniques for real-time exploration. To overcome the lack of scene-scale annotated 4D data and models, especially in panoramic formats, we propose a novel Panoramic Denoiser that adapts generic 2D diffusion priors to animate consistently in 360-degree images, transforming them into panoramic videos with dynamic scenes at targeted regions. Subsequently, we elevate the panoramic video into a 4D immersive environment while preserving spatial and temporal consistency. By transferring prior knowledge from 2D models in the perspective domain to the panoramic domain and the 4D lifting with spatial appearance and geometry regularization, we achieve high-quality Panorama-to-4D generation at a resolution of (4096×2048) for the first time. See the project website at <https://4k4dgen.github.io>.

*Corresponding author.

1 Introduction

With the increasing prevalence of generative techniques [1, 2], the capability to create high-quality assets has the potential to revolutionize content creation across VR/AR and other spatial computing platforms. Unlike 2D displays such as smartphones or tablets, ideal VR/AR content should offer an immersive and seamless experience, supporting 6-DoF virtual tours, such as high-resolution panoramic 4D environments with dynamic scene elements. Despite significant advancements in the generation of images, videos, and 3D models, the development of panoramic 4D content has lagged, primarily due to the scarcity of well-annotated, high-quality 4D training data. Even in the most relevant field of 4D generation, existing works mainly focus on generating or compositing object-level contents [3], which are often in low-resolution (e.g., below 1080p) and cannot fulfill the demand of qualified immersive experiences. Based on these observations, we propose that an ideal generative tool for creating immersive environments should possess the following properties: (i) it should generate content with high perceptual quality, achieving high-resolution (4K) output with dynamic elements (4D); (ii) the 4D representation must be capable of being rendered as coherent, continuous, and seamless 360-degree panoramic views, supporting 6-DoF virtual tours. However, creating diverse 4D panoramic assets of high quality presents two significant challenges: (i) The scarcity of large-scale, annotated 4D data, particularly in panoramic formats, inhibits the training of specialized models. (ii) Achieving both fine-grained local details and global coherence in 4D and 4K panoramic views is challenging for existing 2D diffusion models. These models, typically trained on perspective images with narrow fields of view (FoV), cannot be straightforwardly adapted to the expansive scopes of large panoramic images (see Exp. 4.3). On another front, diffusion models trained with web-scale multi-modal data have demonstrated versatile utility as region-based dynamic priors, and Gaussian Splatting [4] has shown efficient capabilities in modeling 4D environment. Thus, we formulate the 4D panoramic generation problem by animating a static panoramic image into a video, and subsequently elevate the panoramic video into 4D environment assets. Toward this goal, we focus on and address two bottlenecks: (i) the challenge of animating consistent panoramic videos that maintain object dynamics across a 360-degree field-of-view (FoV) using diffusion models originally trained on narrow FoV perspective images, and (ii) the challenge of robustly preserving spatial and temporal consistency as the panoramic video transitions into a 4D environment.

In this paper, we introduce **4K4DGen**, a novel framework designed to facilitate the creation of panoramic 4D environments at resolutions up to 4K. Specifically, we propose the Panoramic Denoiser, which animates specific regions within 360-degree FoV panoramic images by denoising spherical latent codes. This process utilizes a 2D diffusion model initially trained on perspective images with narrow FOV, ensuring global coherence and continuity across the entire panorama. To elevate the omnidirectional panoramic video to a 4D environment, we introduce a 4D lifting mechanism. This mechanism corrects scale discrepancies using a depth estimator enriched with prior knowledge to generate panoramic depth and employs time-dependent 3D Gaussians for cross-frame consistency in dynamic scene representation and rendering. By adapting generic 2D prior models to the panoramic format and effectively lifting 2D dynamics into 4D content with a structured set of 3D Gaussians, we achieve groundbreaking 4K panorama-to-4D content generation. Our contributions can be summarized as follows.

- We introduce the first framework capable of creating high-resolution (up to 4096×2048) 4D omnidirectional assets. This framework addresses the process through two key techniques: panoramic video animation and 4D panoramic lifting. These techniques enable coherent and seamless 4D panoramic rendering, even in the absence of annotated 4D data.
- We propose the Panoramic Denoiser that transfers the generative priors from pre-trained 2D perspective diffusion models to panoramic space, which consistently animate panoramas with scene dynamics.
- We further elevate dynamic panoramic videos into 4D environments using a structured set of 3D Gaussians. Additionally, we have developed a spatial-temporal geometry alignment mechanism that ensures cross-frame consistency and coherence in the 4D environment.

2 Related Work

Diffusion-based Image and Video Generation. Recent advancements have significantly expanded the capabilities of generating 2D images using diffusion models, as evidenced in several studies [5–

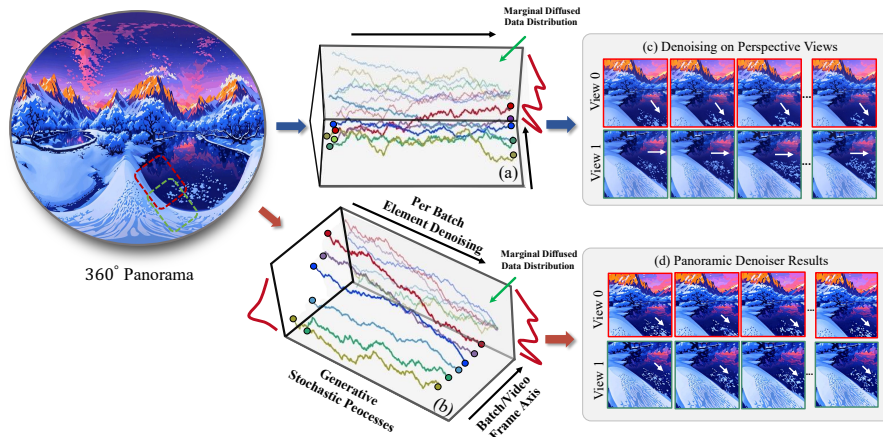


Figure 2: **Panoramic Denoiser.** We propose a method that involves simultaneous denoising of perspective views and their integration into spherical latents at each denoising step. This approach ensures view-consistent animation across different views.

9]. Notably, Stable Diffusion [1] optimizes diffusion models (DMs) within the latent spaces of autoencoders, striking an effective balance between computational efficiency and high image quality. Beyond text conditioning, there is increasing emphasis on integrating additional control signals for more precise image generation [10, 11]. For example, ControlNet [11] enhances the Stable Diffusion encoder to seamlessly incorporate these signals. Furthermore, the generation of multi-view images is gaining attention, with techniques like MVDiffusion [12] processing perspective images with a pre-trained diffusion model. Diffusion models are also extensively applied in video generation, as demonstrated by various recent works [13–18]. For instance, Imagen Video [14] utilizes a series of video diffusion models to generate videos from textual descriptions. Similarly, Make-A-Video [19] advances a diffusion-based text-to-image model to create videos without requiring paired text-video data. MagicVideo [18] employs frame-wise adaptors and a causal temporal attention module for text-to-video synthesis. Video Latent Diffusion Model (VLDM) [20] incorporates temporal layers into a 2D diffusion model to generate temporally coherent videos.

3D/4D Large-scale Generation. In recent 3D computer vision, a large-scale scene is usually represented as implicit or explicit fields for its appearance [4, 21], geometry [22–24], and semantics [25–27]. We mainly discuss the 3D Gaussian Splatting (3DGS) [4] based generation here. Several works including DreamGaussian [28], GaussianDreamer [29], GSGEN [30], and CG3D [31] employ 3DGS to generate diverse 3D objects and lay the foundations for compositionality, while LucidDreamer [32], Text2Immersion [33], GALA3D [34], RealmDreamer [35], and DreamScene360 [36] aim to generate static large-scale 3D scenes from text. Considering the current advancements in 3D generation, investigations into 4D generation using 3DGS representation have also been conducted. DreamGaussian4D [37] accomplishes 4D generation based on a reference image. AYG [38] equips 3DGS with dynamic capabilities through a deformation network for text-to-4D generation. Besides, Efficient4D [39] and 4DGen [40] explore video-to-4D generation, and utilize SyncDreamer [41] to produce multi-view images from input frames as pseudo ground truth for training a dynamic 3DGS.

Panoramic Representation. A panorama is an image that captures a wide, unbroken view of an area, typically encompassing a field of vision much wider than what a standard photo would cover, providing a more immersive representation of the subject. Recently, novel view synthesis using panoramic representation has been widely explored. For instance, PERF [42] trains a panoramic neural radiance field from a single panorama to synthesize 360° novel views. 360Roam [43] proposed learning an omnidirectional neural radiance field and progressively estimating a 3D probabilistic occupancy map to speed up volume rendering. OmniNeRF [44] introduced an end-to-end framework for training NeRF using only 360° RGB images and their approximate poses. PanoHDR-NeRF [45] learns the full HDR radiance field from a low dynamic range (LDR) omnidirectional video by freely moving a standard camera around. In the realm of 3DGS, 360-GS [46] takes 4 panorama images and 2D room layouts as scene priors to reconstruct the panoramic Gaussian radiance field. 4K4D[47] extends 3DGS to high-resolution dynamic scene representation. Most related to our 4K4DGen is DreamScene360 [36], which is a text-to-3D scene generation with a generated 2D panorama as an

intermediate global representation. However, it does not consider dynamics. Our work provides solutions to this problem in the following sections.

3 Methodology

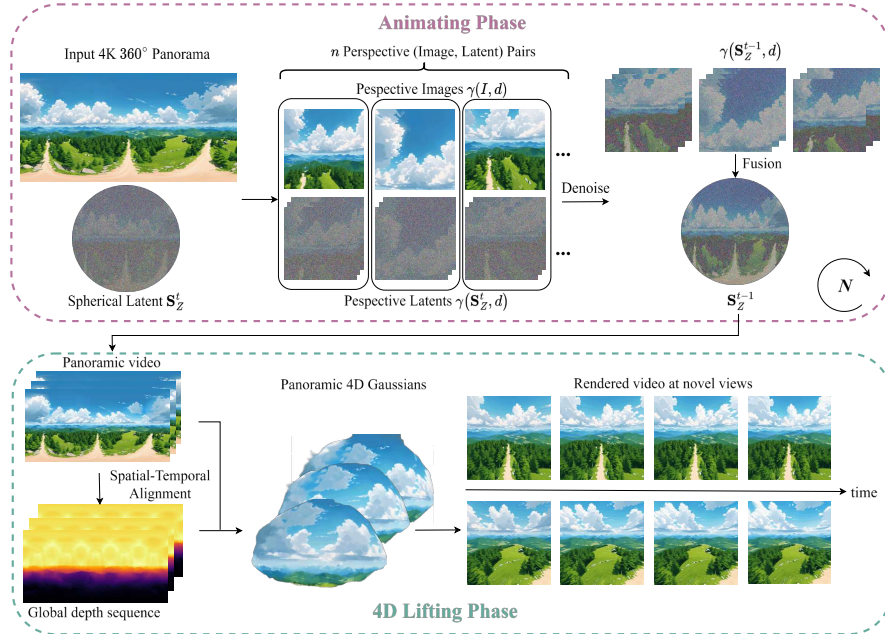


Figure 3: **Overall Pipeline.** Initially, panoramic videos are generated using the Panoramic Denoiser during the animating phase. Subsequently, these videos are transformed into a spatially and temporally consistent 4D representation during the 4D lifting phase.

Taking a single panoramic image as input, the aim of 4K4DGen is to generate a panoramic 4D environment that allows for the rendering of novel views at arbitrary angles and timestamps. Our approach initially constructs a panoramic video and then elevates it to 4D Gaussians, thereby facilitating efficient splatting for flexible rendering. However, naively animating projected perspective images often leads to unnatural motions and inherently inconsistent animations. To address these challenges, our method proposes the denoising of projected spherical latents, thereby enabling consistent animation of the panoramic video from the source image, as detailed in Sec. 3.3. Furthermore, directly converting multiple perspective images from different timestamps into 4D often results in degenerated geometry and noticeable artifacts (see Sec. 4.3); we address this by leveraging spatial-temporal geometry fusion to lift the panoramic video, as described in Sec. 3.4. The entire pipeline of 4K4DGen is illustrated in Fig. 3.

3.1 Preliminaries

Latent Diffusion Models (LDMs). LDMs [48] consist of a forward procedure q and a backward procedure p . The forward procedure gradually introduces noise into the initial latent code $x_0 \in \mathbb{R}^{h \times w \times c}$, where $x_0 = \mathcal{E}(I)$ is the latent code of image I within the latent space of a VAE, denoted by \mathcal{E} . Given the latent code at step $t - 1$, the q procedure is described as $q(x_t|x_{t-1}) = \mathcal{N}(x_t; \sqrt{1 - \beta_t}x_{t-1}, \beta_t I)$. Conversely, the backward procedure p , aimed at progressively removing noise, is defined as $p_\theta(x_{t-1}|x_t) = \mathcal{N}(\mu_\theta(x_t, t), \Sigma_\theta(x_t, t))$. In practical applications, images are generated under the condition y , by progressively sampling from x_T down to x_0 . Recently, image-to-video (I2V) generation has been realized [49, 50] by extending the latent code with an additional frame dimension and performing decoding at each frame. The denoising procedure is succinctly represented as $x_{t-1} = \Phi(x_t, I)$, where $x_t, x_{t-1} \in \mathbb{R}^{l \times h \times w \times c}$ represent the sampled latent codes and I the conditioning image.

Omnidirectional Panoramic Representation. Panoramic images or videos, denoted as I , are represented using equirectangular projections, forming an $H \times W \times C$ matrix where H and W represent the resolution of the image and C is the number of channels. Although this format preserves the matrix structure, aligning with planar images captured by conventional cameras, it introduces distortions, particularly noticeable at the polar regions of the projected image. To address this, we adopt a spherical representation for panoramas, defining pixel values on a sphere $\mathbb{S}^2 = \{\mathbf{d} = (x, y, z) | x, y, z \in \mathbb{R} \wedge |\mathbf{d}| = 1\}$. For a formal definition of the projection, we employ a mapping $\mathcal{E}_I : [-1, 1]^2 \rightarrow \mathbb{R}^C$, normalizing the image coordinates into the range $[0, 1]$. Therefore, for a given pixel $(x, y) \in [-1, 1]^2$, the corresponding pixel value is derived from $\mathcal{E}_I(x, y)$. We define the spherical representation of panoramas using the field $\mathcal{S}_I : \mathbb{S}^2 \rightarrow \mathbb{R}^C$, where $\mathcal{S}_I(\mathbf{d})$ gives the pixel value at a given direction $\mathbf{d} = (x, y, z)$. The relationship between the spherical and equirectangular representations is established through the following projection formula:

$$\mathcal{S}_I(x, y, z) = \mathcal{E}_I\left(\frac{1}{\pi} \arccos \frac{y}{\sqrt{1-z^2}}, \frac{2}{\pi} \arcsin z\right). \quad (1)$$

For perspective images, we establish a virtual camera centered at the origin. The rays for all pixels are defined through ray casting, as described in [21], where each ray \mathbf{d} is represented by $\mathbf{r}(x, y, f, \mathbf{u}, \mathbf{s}, R)$. This representation considers the focal length f , the z-axis direction \mathbf{u} , the image plane size \mathbf{s} , and the camera rotation along the z-axis R . Consequently, for a given panorama I , the perspective image P can be projected using these camera parameters $(f, \mathbf{u}, \mathbf{s}, R)$ as:

$$\mathcal{E}_P(x, y) = \mathcal{S}_I \circ \mathbf{r}(x, y, f, \mathbf{u}, \mathbf{s}, R). \quad (2)$$

In this paper, we fix the focal length f , image plane size \mathbf{s} , and the rotation R . We denote the process of projecting the panorama I into a perspective image i , based on the camera's z-axis direction \mathbf{u} , as $i = \gamma(I, \mathbf{u})$.

3.2 Inconsistent Perspective Animation

Large-scale pre-trained 2D models have demonstrated impressive generative capabilities in producing images and videos, leveraging massive multi-modal training data sourced from the Internet. However, collecting high-quality 4D training data is non-trivial, and no existing 4D dataset matches the scale of those available for images and videos. Therefore, our approach aims to utilize the capabilities of video generative models to produce consistent panoramic 360-degree videos, which are then elevated to 4D. Nonetheless, the availability of panoramic videos is significantly more limited compared to planar perspective videos. Consequently, mainstream image-to-video (I2V) animation techniques may not perform optimally on panoramic formats, and the resolution of the videos remains constrained, as illustrated in Fig. 6 (b) and Tab. 2. Alternatively, the animator can be applied to perspective images. However, this method results in inconsistencies among different projected views, as illustrated in Fig. 6 (c).

3.3 Consistent Panoramic Animation

Limited by the scarcity of 4D training data in panoramic format, and given that large diffusion models are primarily trained on planar perspective videos, directly applying 2D perspective denoisers poses challenges due to inconsistent motion between different perspective views. This limitation has motivated us to develop a panoramic video generator that utilizes priors from image-to-video (I2V) animators, which are predominantly trained on planar perspective image-video pairs. Consequently, given a static input panorama, we animate it into a panoramic video, as demonstrated in the "Animating Phase" section of Fig. 3.

Spherical Latent Space. To generate panoramic video from a static panorama, we adopt the denoise-in-latent-space schema utilized in latent diffusion models [2, 50, 51]. Initially, a noisy latent code is sampled, which is then progressively denoised using the DDPM procedure [52]. Throughout each step of this denoising process, the static input image serves as a conditioning term. Finally, the clean latent code is decoded by a pre-trained VAE decoder to render the video in pixel space. In 4K4DGen, unlike the method for generating perspective planar videos, both the latent code and the input static panorama are represented on spheres. We start with the initial panoramic latent code $S^T : \mathbb{S}^2 \rightarrow \mathbb{R}^{L \times c}$, where L denotes the number of video frames and c the channels per frame. A novel Panoramic Denoiser then generates the clean panoramic latent code S^0 , conditioned on the

static input panorama $I \in \mathbb{R}^{H \times W}$. Subsequently, the equirectangular projection, as introduced in Sec. 3.1, projects the clean panoramic latent code into the matrix-like latent code $Z^0 \in \mathbb{R}^{h \times w \times L \times c}$, with h and w representing the resolution of the latent code. Each k^{th} video frame I^k in pixel space is decoded by the pre-trained VAE decoder as $I^k = \mathcal{D}(Z^0[:, :, k, :])$.

Build the Panoramic Denoiser. We employ a pre-trained perspective video generative model [50] to develop our Panoramic Denoiser. This video generator takes a perspective image $i \in \mathbb{R}^{p_H \times p_W \times c}$ and an initial latent code $z^T \in \mathbb{R}^{p_h \times p_w \times (L \times c)}$ as inputs. It then progressively denoises the latent code z^T to a noise-free state z^0 using a denoising function $z^{t-1} = \Phi(z^t, i)$, where p_h, p_w are the resolutions of the latent code, p_H, p_W are the dimensions of the conditioning image, c is the number of channels, and L represents the video length. Our goal is to transform the initial noisy latent code S^T into the clean panoramic latent code S^0 , ensuring that each perspective view is appropriately animated while maintaining global consistency. The underlying intuition is that if each perspective view undergoes its respective denoising process, the perspective video will feature meaningful animation. Moreover, if two perspective views overlap, they will align with each other [53, 54] to produce a seamless global animation. Given a static input panorama I and an initial spherical latent code $S^0 : \mathbb{S}^2 \rightarrow \mathbb{R}^{L \times c}$, we progressively remove noise employing a project-and-fuse procedure at each denoising step. Specifically, the spherical latent code at the t^{th} denoising step, $S^t : \mathbb{S}^2 \rightarrow \mathbb{R}^{L \times c}$, is projected into multiple perspective latent codes $\mathcal{Z}^t = \{z_1^t, z_2^t, \dots, z_n^t\}$, where each $z_k^t = \gamma(S^t, \mathbf{d}_k) \in \mathbb{R}^{p_h \times p_w \times (L \times c)}$ represents the k^{th} perspective latent code projected in the equirectangular format detailed in Sec. 3.1. Each perspective latent code is then denoised by one step using a pre-trained perspective denoiser, denoted as $z_k^{t-1} = \Phi(z_k^t, i_k)$, where $i_k = \gamma(I, \mathbf{d}_k) \in \mathbb{R}^{p_H \times p_W \times c}$ is the perspective conditioning image projected from the panorama I . Subsequently, we optimize the spherical latent code $S^{t-1} : \mathbb{S}^2 \rightarrow \mathbb{R}^{L \times c}$ at step $t-1$ by fusing all the denoised perspective latent codes z_k^{t-1} . Formally, the denoising procedure at step t , denoted as $S^{t-1} = \Psi(S^t, I)$, encompasses the following operations:

$$\Psi(S^t, I) = \underset{\mathcal{S}}{\operatorname{argmin}} \mathbb{E}_{\mathbf{d} \in \mathbb{S}^2} \|\gamma(\mathcal{S}, \mathbf{d}) - \Phi(\gamma(S^t, \mathbf{d}), \gamma(I, \mathbf{d}))\|. \quad (3)$$

3.4 Panoramic 4D Lifting

We define the panoramic video as $V = \{I^1, I^2, \dots, I^L\}$, consisting of L frames. The video is divided into overlapping perspective videos $\{v_0, v_1, \dots, v_n\}$, each captured from specific camera directions $\{\mathbf{d}_1, \dots, \mathbf{d}_n\}$, collectively encompassing the entire span of the panoramic video V . Subsequently, we estimate the geometry of the 4D scene by fusing the depth maps through spatial-temporal geometry alignment. Following this, we describe our methodology for 4D representation and the subsequent rendering procedure.

Supervision from Spatial-Temporal Geometry Alignment. To transition from 2D video to 3D space, we utilize a monocular depth estimator [55], inspired by advancements in [36], to estimate the scene’s geometric structure. Nonetheless, depth maps generated for each frame and perspective might lack spatial and temporal consistency. To address this, we implement Spatial-Temporal Geometry Alignment using a pre-trained depth estimator $\Theta : \mathbb{R}^{h \times w \times 3} \rightarrow \mathbb{R}^{h \times w}$, applied to perspective images. Our objective is to amalgamate n perspective depth maps $D_i^K = \Theta(\gamma(I^k, \mathbf{d}_i))$ into a cohesive panoramic depth map D^k for each frame I^k , ensuring spatial and temporal continuity. We express these depth maps as a spherical representation S_D^1, \dots, S_D^L . For enhanced optimization, we assign n scale factors $\alpha_i^k \in \mathbb{R}$ and shifting parameters $\beta_i^k \in \mathbb{R}^{h \times w}$ to each perspective depth map. The comprehensive depth map D^k is then optimized jointly with these parameters α and β . The formal objective is structured as follows:

$$S_D^k = \underset{\mathcal{S}}{\operatorname{argmin}} \mathbb{E}_{i \in \{1, \dots, n\}} \lambda_{\text{depth}} \mathcal{L}_{\text{depth}} + \lambda_{\text{scale}} \mathcal{L}_{\text{scale}} + \lambda_{\text{shift}} \mathcal{L}_{\text{shift}}. \quad (4)$$

where $\mathcal{L}_{\text{depth}} = \|\text{softplus}(\alpha_i^k) \Theta(\gamma(I^k, \mathbf{d}_i)) - \gamma(\mathcal{S}) + \beta_i^k\|$ is the depth supervision term, $\mathcal{L}_{\text{scale}} = \|\alpha_i^k - \alpha_i^{k-1}\| + \|\text{softplus}(\alpha_i^k) - 1\|$ the regularize term for α , and $\mathcal{L}_{\text{shift}} = \mathcal{L}_{\text{TV}}(\beta_i^k) + \|\beta_i^k - \beta_i^{k-1}\|$ the regularize term for β where \mathcal{L}_{TV} is the TV regularization.

4D Representation and Rendering. We represent and render the dynamic scene using T sets of 3D Gaussians. Each set, corresponding to a specific timestamp t , is denoted as $G_t =$

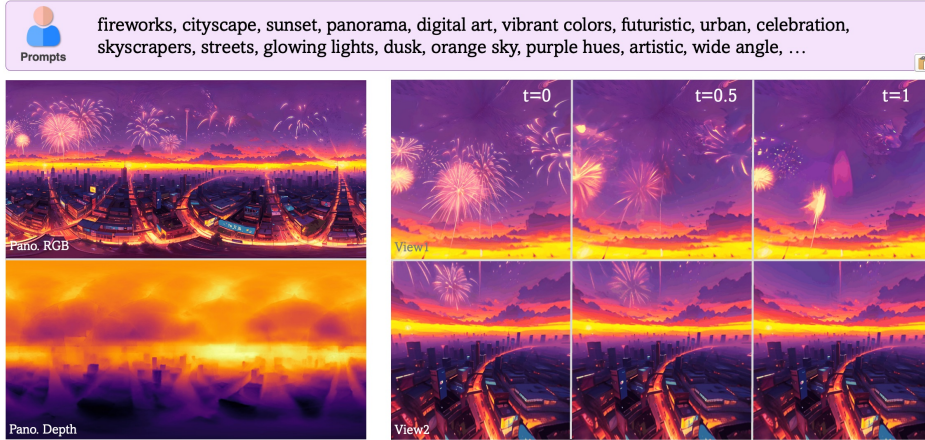


Figure 4: **Visualization Results for 4K4DGen.** Displayed are the input panorama (Pano. RGB), the optimized global geometry (Pano. Depth), and the final rendered results. For each panorama, we illustrate the rendered video and depth frames from three timestamps ($t = 0, t = 0.5, t = 1$), captured from two overlapping views (View1, View2). 4K4DGen effectively generates 4D scenes that are both spatially and temporally consistent.

$\{(p_t^i, q_t^i, s_t^i, c_t^i, o_t^i) \mid i = 1, \dots, n\}$. This definition aligns with the methods described in [3], which also provides a fast rasterizer for rendering images based on these Gaussian sets and given camera parameters. Consistent with Sec. 3.1, while the camera intrinsics remain fixed, we parameterize the camera extrinsics through a position $\mathbf{p} \in \mathbb{R}^3$ and an orientation $\mathbf{d} \in \mathbb{S}^2$. The training process is structured in two stages: initially, we directly supervise the 3D Gaussians using the panoramic videos. Let $\mathcal{R}(G, \mathbf{p}, \mathbf{d})$ represent the rasterized image from Gaussian set G , utilizing camera extrinsics $\mathbf{p} = \mathbf{0}$ and camera direction \mathbf{d} . Let I_t denote the t^{th} frame of the panoramic video. We optimize the t^{th} Gaussian set G_t using the following objective:

$$\mathcal{L} = \lambda_{\text{rgb}} \mathcal{L}_{\text{rgb}} + \lambda_{\text{temporal}} \mathcal{L}_{\text{temporal}} + \lambda_{\text{sem}} \mathcal{L}_{\text{sem}} + \lambda_{\text{geo}} \mathcal{L}_{\text{geo}} \quad (5)$$

where the RGB supervision term $\mathcal{L}_{\text{rgb}} = \lambda \mathcal{L}_1 + (1 - \lambda) \mathcal{L}_{\text{SSIM}}$ is the same as 3D-GS [4], and the temporal regularize term $\mathcal{L}_{\text{temporal}}$ written as:

$$\mathcal{L}_{\text{temporal}} = \sum_{i=1}^n \|\mathcal{R}(G_t, \mathbf{0}, \mathbf{d}_i) - \mathcal{R}(G_{t-1}, \mathbf{0}, \mathbf{d}_i)\| \quad (6)$$

In the second stage, we adopt the distillation loss and geometric regularization used in [36], the distillation loss is defined as follows: $\mathcal{L}_{\text{sem}} = 1 - \cos \langle \text{CLS}(\mathcal{R}(G_t, \mathbf{0}, \mathbf{d}_i)), \text{CLS}(\mathcal{R}(G_t, \delta_p, \mathbf{d}_i)) \rangle$, where $\delta_p \in [-\alpha, \alpha]^3$ is the disturbing vector, $\text{CLS}(\cdot)$ the feature extractor such as DINO [56], and $\cos \langle \cdot, \cdot \rangle$ the cos value of two vectors. The geometric regularization is defined as follows: $\mathcal{L}_{\text{geo}} = 1 - \frac{\text{Cov}(\mathcal{R}_D(G_t, \mathbf{0}, \mathbf{d}_i), \Theta(\gamma(I, \mathbf{d}_i)))}{\sqrt{\text{Var}(\mathcal{R}_D(G_t, \mathbf{0}, \mathbf{d}_i)) \text{Var}(\Theta(\gamma(I, \mathbf{d}_i)))}}$, where \mathcal{R}_D is the rendered depth, $\text{Cov}(\cdot, \cdot)$ the covariance, and $\text{Var}(\cdot)$ the variance.

4 Experiments

4.1 Experimental Settings

Implementation Details. We begin by detailing the acquisition of panoramas utilized in our experiments. These panoramas are generated from text prompts using state-of-the-art generative models [57–59], initially at a resolution of 6144×3072 . Subsequently, these images are resized to 4096×2048 or 2048×1024 . We further delineate the spherical representation details by selecting 20 uniform directions \mathbf{u} on the sphere \mathbb{S}^2 . In every experiment, the image plane size \mathbf{s} is maintained at 0.6×0.6 , with a focal length $f = 0.6$ and a resolution of 512×512 . Rotation along the z-axis is set to zero for all cameras, ensuring that the up-axis for the i^{th} camera aligns with the $(O, \mathbf{d}_i, \mathbf{z})$ plane.

During the animating phase, we employ the perspective denoiser Φ , instantiated as the Animate-anything model [50], which fine-tunes the SVD model [2]. In the Spatial-Temporal Geometric Alignment stage of the Lifting phase, the depth estimator Θ is represented by MiDaS [55, 60]. Crucially, the depth map from the perspective image is adjusted by a scaling factor, corresponding to the projection of the unit-length ray direction onto the camera orientation d . For scenes without boundaries, depth values for distant elements, such as the sky, are set to a finite number to facilitate optimization. The hyper-parameters are set as follows: $\lambda_{\text{depth}} = 1$, $\lambda_{\text{scale}} = 0.1$, $\lambda_{\text{shift}} = 0.01$. We conduct Spatial-Temporal Geometry Alignment optimization over 3000 iterations, with λ_{scale} and λ_{shift} set to zero during the first 1500 iterations. For the 4D representation training stage, Gaussian parameters are optimized over 10000 iterations for each time stamp t . The hyper-parameters for this stage are defined as $\lambda_{\text{rgb}} = 1$, $\lambda_{\text{temporal}} = \lambda_{\text{sem}} = \lambda_{\text{geo}} = 0.05$, and the disturbance vector range α is varied at 0.05, 0.1, and 0.2 during the 5400, 6600, and 9000 iterations, respectively. All experiments are executed on a single NVIDIA A100 GPU with 80 GB RAM.

Evaluation. As there are no ground truth 4D scenes available, we render videos at specific test camera poses from the synthesized 4D representation and employ non-reference video/image quality assessment methods for quantitative evaluation of our approach. For the test views, we select random cameras with $p = 0$ as part of our testing camera set. We then introduce disturbances as described in Sec. 3.4, applying a disturbance factor of $\alpha = 0.05$ at these selected views. **Datasets.** The task of generating 4D panoramas from static panoramas is novel, and thus, no pre-existing datasets are available. We assess our methodology using panoramas generated by text-to-panorama diffusion models, comprising a dataset of 16 panoramas. **Baselines.** Current SDS-based methods [61, 62] are limited to generating object-centered assets and do not support the generation of outward-facing scenes. We compare our method with the optical-flow-based 3D dynamic image technique, 3D-Cinematography (3D-Cin.) [63], by inputting the panorama into 3D-Cin. and projecting its output onto perspective images. **Metrics.** We assess video consistency using the CLIP consistency score, which averages the CLIP distances of consecutive frames, and the CLIP-I score, which evaluates the distance of each frame relative to the input panorama. Additionally, a user study is conducted where participants are solicited to vote for the video they perceive as superior in quality or decide whether two views are consistent with each other.

4.2 Results

Comparison to Baselines. We present both qualitative and quantitative comparisons of 4K4DGen to 3D-Cinematography in Fig. 5 and Tab. 1. The figure illustrates that 4K4DGen generates results of superior quality. According to the data presented in the table, 4K4DGen not only achieves higher CLIP similarity scores but also receives more favorable evaluations from users regarding its quality.

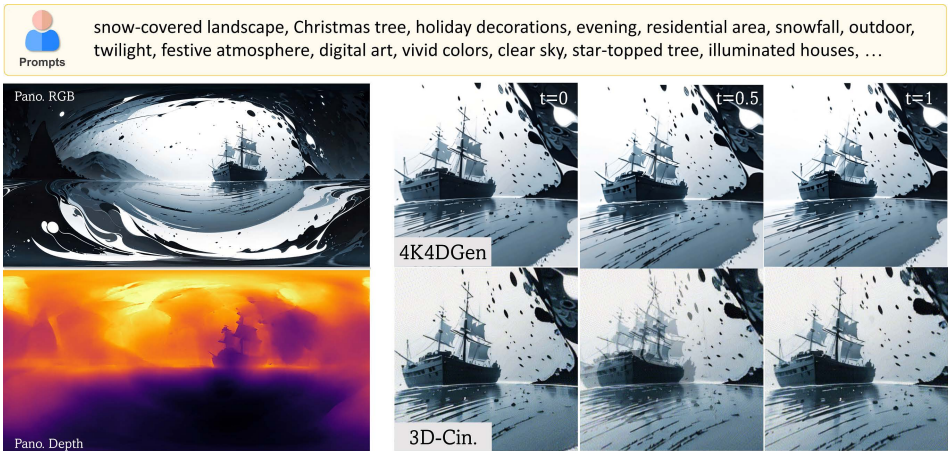


Figure 5: **Comparison between 4K4DGen and 3D-Cinematography.** 3D-Cinematography produces ghost images at the middle frame.

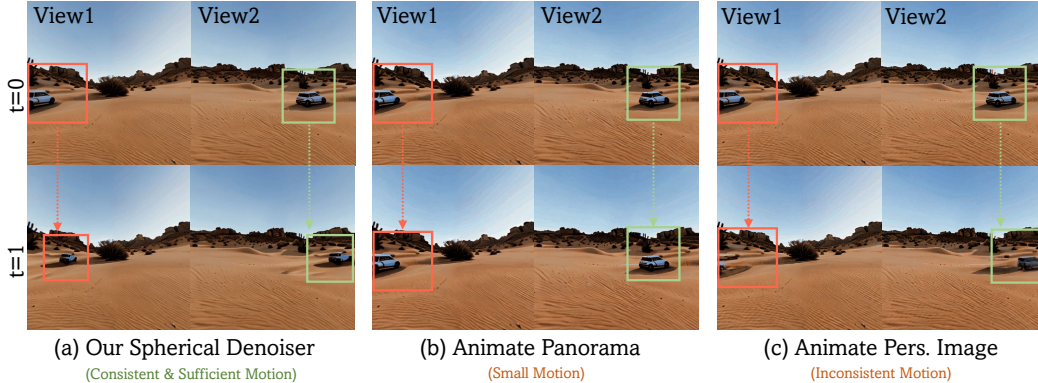


Figure 6: **Comparison to Different Animators:** An animator primarily trained on perspective images, when applied to panoramas, is likely to generate minor motion, and the resolution may be limited. Conversely, animating perspective images can result in inconsistencies between different views.

Visualization Results. Additional visualization results, encompassing both rendered images and depth maps, are displayed in Figure 4. These qualitative results demonstrate that 4K4DGen can effectively generate 4D panoramic scenes that are both spatially and temporally consistent. This capability significantly enhances the immersive experience on VR devices.

4.3 Ablation Studies

We perform ablation studies for both the animating and lifting phases of our methodology. During the animating phase, we demonstrate the critical role of our spherical denoise strategy by substituting it with two basic animation strategies. In the lifting phase, we examine the effects of omitting the Spatial-Temporal Geometry Alignment process and the temporal loss in optimizing 4D representations.

Animating Phase. To animate the panorama into a panoramic video, a naive approach is to apply animators directly to the entire panorama. However, we observed that this strategy often results in minor motion, as shown in Fig. 6 (b) and Tab. 2 (Animate Pano.). This issue arises due to two main reasons: (1) animators are typically trained on perspective images with a narrow field of view (FoV), whereas panoramas have a 360-degree FoV with specific distortions under the equirectangular projection; (2) our panorama is high-resolution (4K), which exceeds the training distribution of most 2D animators and can easily cause out-of-memory issues, even with an 80GB VRAM graphics card. Thus we have to resize the panorama to a small resolution (2k), causing a loss of details. Thus, we seek to animate on perspective views. Applying the animator to perspective views offers benefits such as reduced distortion and domain-appropriate input for the animator, allowing for smooth animation of high-resolution panoramas. However, animating perspective images separately can introduce inconsistencies between overlapping perspective views, as illustrated in Fig. 6 (c) and Tab. 2 (Animate Pers.). To resolve this challenge, we propose simultaneously denoising all perspective views and fusing them at each denoising step, which capitalizes on the benefits of animating perspective views while ensuring cross-view consistency. The results are displayed in Fig. 6 (a) and Tab. 2 (Ours).

Table 1: **Comparison with 3D-Cinematography.** Our method, 4K4DGen, consistently achieves higher CLIP similarity scores compared to the same panorama image processed by 3D-Cinematography. Furthermore, the majority of participants in our user study rated the visual quality of 4K4DGen as superior.

Method	CLIP(Consistency) \uparrow	CLIP-I \uparrow	User Vote \uparrow
3D-Cinematography [63]	0.98	0.96	19%
4K4DGen	0.99	0.98	81%

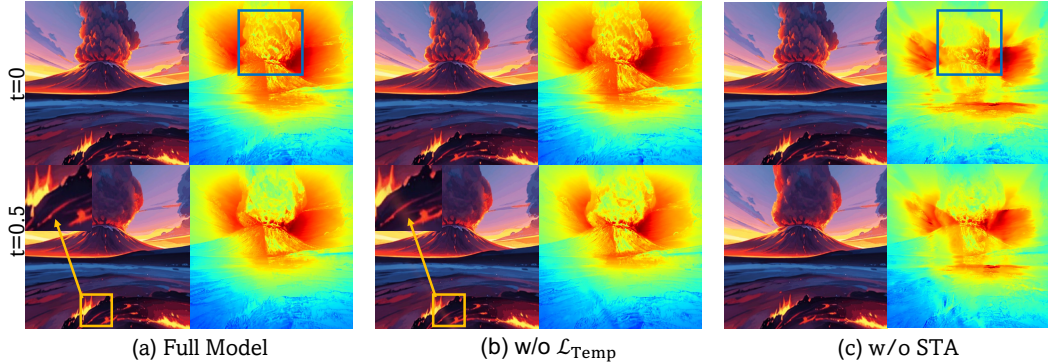


Figure 7: **Ablation of the Lifting Phase.** Omitting temporal regularization during the optimization of 3D Gaussians results in the appearance of artifacts. The absence of Spatial-Temporal Geometry Alignment causes the degradation of geometric structures.

Lifting Phase. We conduct ablation studies on the Spatial-Temporal Geometry Alignment (STA) module and the temporal loss during the lifting phase. Our findings indicate that removing the STA module leads to a degradation in geometric quality, as shown in Fig. 7 (c). Additionally, omitting the temporal loss introduces artifacts in certain frames, potentially resulting in flickering, as demonstrated in Fig. 7 (b).

Table 2: **Different Animation Strategies in the Animating Phase.** Animating the entire panorama results in minor motion and reduced resolution (first row). Conversely, animating from perspective views leads to inconsistencies across different views (second row). This is supported by user feedback, where 70% of participants identified our method as view-consistent, in contrast to only 33% who found animation from perspective views to be view-consistent.

Animator	Max Pano. Res.	CLIP \uparrow	Motion \uparrow	View-consistency (User Vote) \uparrow
Animate Pano.	2048 \times 1024	<u>0.983</u>	0.30	-
Animate Pers.	4096 \times 2048	0.985	<u>0.91</u>	<u>33%</u>
Ours	4096 \times 2048	0.979	1.27	70%

5 Conclusion, Limitation and Broader Impact

Conclusion. We have proposed a novel framework **4K4DGen**, allowing users to create high-quality 4K panoramic 4D content using text prompts, which delivers immersive virtual touring experiences. To achieve panorama-to-4D even without high-quality 4D training data, we integrate generic 2D prior models into the panoramic domain. Our approach involves a two-stage pipeline: initially generating panoramic videos using a Panoramic Denoiser, followed by 4D elevation through a Spatial-Temporal Geometry Alignment mechanism to ensure spatial coherence and temporal continuity.

Limitation. First, the quality of temporal animation in the generated 4D environment mainly relies on the ability of the pre-trained I2V model. Future improvements could include the integration of a more advanced 2D animator. Second, since our method ensures spatial and temporal continuity during the 4D elevation phase, it is currently unable to synthesize significant changes in the environment, such as the appearance of glowing fireflies or changing weather conditions. Third, the high-resolution and time-dependent representation of the generated 4D environment necessitates substantial storage capacity, which could be optimized in future work using techniques such as model distillation and pruning.

Broader Impact. Our research enables the generation of 4D digital scenes from a single panoramic image, which is advantageous for various applications such as AR/VR, movie production, and video games. This technology distinctly excels in creating high-resolution 4D scenes up to 4K, significantly enhancing user experiences. However, there is potential for misuse in the creation of deceptive content or privacy violations, which contradicts our ethical intentions. These risks can be mitigated through a combination of regulatory and technical strategies, such as watermarking.

References

- [1] Robin Rombach, Andreas Blattmann, Dominik Lorenz, Patrick Esser, and Björn Ommer. High-resolution image synthesis with latent diffusion models. In *Proceedings of the IEEE/CVF conference on computer vision and pattern recognition*, pages 10684–10695, 2022.
- [2] Andreas Blattmann, Tim Dockhorn, Sumith Kulal, Daniel Mendelevitch, Maciej Kilian, Dominik Lorenz, Yam Levi, Zion English, Vikram Voleti, Adam Letts, et al. Stable video diffusion: Scaling latent video diffusion models to large datasets. *arXiv preprint arXiv:2311.15127*, 2023.
- [3] Sherwin Bahmani, Ivan Skorokhodov, Victor Rong, Gordon Wetzstein, Leonidas Guibas, Peter Wonka, Sergey Tulyakov, Jeong Joon Park, Andrea Tagliasacchi, and David B Lindell. 4d-fy: Text-to-4d generation using hybrid score distillation sampling. *arXiv preprint arXiv:2311.17984*, 2023.
- [4] Bernhard Kerbl, Georgios Kopanas, Thomas Leimkühler, and George Drettakis. 3d gaussian splatting for real-time radiance field rendering. *ACM Transactions on Graphics*, 42(4):1–14, 2023.
- [5] Prafulla Dhariwal and Alexander Nichol. Diffusion models beat gans on image synthesis. *Advances in neural information processing systems*, 34:8780–8794, 2021.
- [6] Alex Nichol, Prafulla Dhariwal, Aditya Ramesh, Pranav Shyam, Pamela Mishkin, Bob McGrew, Ilya Sutskever, and Mark Chen. Glide: Towards photorealistic image generation and editing with text-guided diffusion models. *arXiv preprint arXiv:2112.10741*, 2021.
- [7] Dustin Podell, Zion English, Kyle Lacey, Andreas Blattmann, Tim Dockhorn, Jonas Müller, Joe Penna, and Robin Rombach. Sdxl: Improving latent diffusion models for high-resolution image synthesis. *arXiv preprint arXiv:2307.01952*, 2023.
- [8] Aditya Ramesh, Prafulla Dhariwal, Alex Nichol, Casey Chu, and Mark Chen. Hierarchical text-conditional image generation with clip latents. *arXiv preprint arXiv:2204.06125*, 1(2):3, 2022.
- [9] Chitwan Saharia, William Chan, Saurabh Saxena, Lala Li, Jay Whang, Emily L Denton, Kamyar Ghasemipour, Raphael Gontijo Lopes, Burcu Karagol Ayan, Tim Salimans, et al. Photorealistic text-to-image diffusion models with deep language understanding. *Advances in neural information processing systems*, 35:36479–36494, 2022.
- [10] Chong Mou, Xintao Wang, Liangbin Xie, Jian Zhang, Zhongang Qi, Ying Shan, and Xiaohu Qie. T2i-adapter: Learning adapters to dig out more controllable ability for text-to-image diffusion models. *arXiv e-prints*, pages arXiv–2302, 2023.
- [11] Lvmin Zhang, Anyi Rao, and Maneesh Agrawala. Adding conditional control to text-to-image diffusion models. In *Proceedings of the IEEE/CVF International Conference on Computer Vision*, pages 3836–3847, 2023.
- [12] Shitao Tang, Fuyang Zhang, Jiacheng Chen, Peng Wang, and Yasutaka Furukawa. Mvdifffusion: Enabling holistic multi-view image generation with correspondence-aware diffusion. *arXiv*, 2023.
- [13] Songwei Ge, Seungjun Nah, Guilin Liu, Tyler Poon, Andrew Tao, Bryan Catanzaro, David Jacobs, Jia-Bin Huang, Ming-Yu Liu, and Yogesh Balaji. Preserve your own correlation: A noise prior for video diffusion models. In *Proceedings of the IEEE/CVF International Conference on Computer Vision*, pages 22930–22941, 2023.
- [14] Jonathan Ho, William Chan, Chitwan Saharia, Jay Whang, Ruiqi Gao, Alexey Gritsenko, Diederik P Kingma, Ben Poole, Mohammad Norouzi, David J Fleet, et al. Imagen video: High definition video generation with diffusion models. *arXiv preprint arXiv:2210.02303*, 2022.
- [15] Jiuniu Wang, Hangjie Yuan, Dayou Chen, Yingya Zhang, Xiang Wang, and Shiwei Zhang. Modelscope text-to-video technical report. *arXiv preprint arXiv:2308.06571*, 2023.
- [16] Jay Zhangjie Wu, Yixiao Ge, Xintao Wang, Stan Weixian Lei, Yuchao Gu, Yufei Shi, Wynne Hsu, Ying Shan, Xiaohu Qie, and Mike Zheng Shou. Tune-a-video: One-shot tuning of image diffusion models for text-to-video generation. In *Proceedings of the IEEE/CVF International Conference on Computer Vision*, pages 7623–7633, 2023.
- [17] Ruiqi Wu, Liangyu Chen, Tong Yang, Chunle Guo, Chongyi Li, and Xiangyu Zhang. Lamp: Learn a motion pattern for few-shot-based video generation. *arXiv preprint arXiv:2310.10769*, 2023.

- [18] Daquan Zhou, Weimin Wang, Hanshu Yan, Weiwei Lv, Yizhe Zhu, and Jiashi Feng. Magicvideo: Efficient video generation with latent diffusion models. *arXiv preprint arXiv:2211.11018*, 2022.
- [19] Uriel Singer, Adam Polyak, Thomas Hayes, Xi Yin, Jie An, Songyang Zhang, Qiuyan Hu, Harry Yang, Oron Ashual, Oran Gafni, et al. Make-a-video: Text-to-video generation without text-video data. *arXiv preprint arXiv:2209.14792*, 2022.
- [20] Andreas Blattmann, Robin Rombach, Huan Ling, Tim Dockhorn, Seung Wook Kim, Sanja Fidler, and Karsten Kreis. Align your latents: High-resolution video synthesis with latent diffusion models. In *Proceedings of the IEEE/CVF Conference on Computer Vision and Pattern Recognition*, pages 22563–22575, 2023.
- [21] Ben Mildenhall, Pratul P. Srinivasan, Matthew Tancik, Jonathan T. Barron, Ravi Ramamoorthi, and Ren Ng. Nerf: Representing scenes as neural radiance fields for view synthesis. In *ECCV*, 2020.
- [22] Songyou Peng, Michael Niemeyer, Lars Mescheder, Marc Pollefeys, and Andreas Geiger. Convolutional occupancy networks. In *Computer Vision—ECCV 2020: 16th European Conference, Glasgow, UK, August 23–28, 2020, Proceedings, Part III 16*, pages 523–540. Springer, 2020.
- [23] Zhen Wang, Shijie Zhou, Jeong Joon Park, Despoina Paschalidou, Suyu You, Gordon Wetzstein, Leonidas Guibas, and Achuta Kadambi. Alto: Alternating latent topologies for implicit 3d reconstruction. In *Proceedings of the IEEE/CVF Conference on Computer Vision and Pattern Recognition*, pages 259–270, 2023.
- [24] Jiahui Huang, Zan Gojcic, Matan Atzmon, Or Litany, Sanja Fidler, and Francis Williams. Neural kernel surface reconstruction. In *Proceedings of the IEEE/CVF Conference on Computer Vision and Pattern Recognition*, pages 4369–4379, 2023.
- [25] Justin Kerr, Chung Min Kim, Ken Goldberg, Angjoo Kanazawa, and Matthew Tancik. Lurf: Language embedded radiance fields. In *Proceedings of the IEEE/CVF International Conference on Computer Vision*, pages 19729–19739, 2023.
- [26] Shijie Zhou, Haoran Chang, Sicheng Jiang, Zhiwen Fan, Zehao Zhu, Dejia Xu, Pradyumna Chari, Suyu You, Zhangyang Wang, and Achuta Kadambi. Feature 3dgs: Supercharging 3d gaussian splatting to enable distilled feature fields. *Proceedings of the IEEE/CVF Conference on Computer Vision and Pattern Recognition*, 2024.
- [27] Minghan Qin, Wanhua Li, Jiawei Zhou, Haoqian Wang, and Hanspeter Pfister. Langsplat: 3d language gaussian splatting. *arXiv preprint arXiv:2312.16084*, 2023.
- [28] Jiaying Tang, Jiawei Ren, Hang Zhou, Ziwei Liu, and Gang Zeng. Dreamgaussian: Generative gaussian splatting for efficient 3d content creation. *arXiv preprint arXiv:2309.16653*, 2023.
- [29] Taoran Yi, Jiemin Fang, Guanjuan Wu, Lingxi Xie, Xiaopeng Zhang, Wenyu Liu, Qi Tian, and Xinggang Wang. Gaussiandreamer: Fast generation from text to 3d gaussian splatting with point cloud priors. *arXiv preprint arXiv:2310.08529*, 2023.
- [30] Zilong Chen, Feng Wang, and Huaping Liu. Text-to-3d using gaussian splatting. *arXiv preprint arXiv:2309.16585*, 2023.
- [31] Alexander Vilesov, Pradyumna Chari, and Achuta Kadambi. Cg3d: Compositional generation for text-to-3d via gaussian splatting. *arXiv preprint arXiv:2311.17907*, 2023.
- [32] Jaeyoung Chung, Suyoung Lee, Hyeongjin Nam, Jaerin Lee, and Kyoung Mu Lee. Luciddreamer: Domain-free generation of 3d gaussian splatting scenes. *arXiv preprint arXiv:2311.13384*, 2023.
- [33] Hao Ouyang, Kathryn Heal, Stephen Lombardi, and Tiancheng Sun. Text2immersion: Generative immersive scene with 3d gaussians. *arXiv preprint arXiv:2312.09242*, 2023.
- [34] Xiaoyu Zhou, Xingjian Ran, Yajiao Xiong, Jinlin He, Zhiwei Lin, Yongtao Wang, Deqing Sun, and Ming-Hsuan Yang. Gala3d: Towards text-to-3d complex scene generation via layout-guided generative gaussian splatting. *arXiv preprint arXiv:2402.07207*, 2024.
- [35] Jaidev Shriram, Alex Trevithick, Lingjie Liu, and Ravi Ramamoorthi. Realdreamer: Text-driven 3d scene generation with inpainting and depth diffusion. *arXiv preprint arXiv:2404.07199*, 2024.
- [36] Shijie Zhou, Zhiwen Fan, Dejia Xu, Haoran Chang, Pradyumna Chari, Tejas Bharadwaj, Suyu You, Zhangyang Wang, and Achuta Kadambi. Dreamscene360: Unconstrained text-to-3d scene generation with panoramic gaussian splatting. *arXiv preprint arXiv:2404.06903*, 2024.

- [37] Jiawei Ren, Liang Pan, Jiaxiang Tang, Chi Zhang, Ang Cao, Gang Zeng, and Ziwei Liu. Dreamgaussian4d: Generative 4d gaussian splatting. *arXiv preprint arXiv:2312.17142*, 2023.
- [38] Huan Ling, Seung Wook Kim, Antonio Torralba, Sanja Fidler, and Karsten Kreis. Align your gaussians: Text-to-4d with dynamic 3d gaussians and composed diffusion models. *arXiv preprint arXiv:2312.13763*, 2023.
- [39] Zijie Pan, Zeyu Yang, Xiatian Zhu, and Li Zhang. Fast dynamic 3d object generation from a single-view video. *arXiv preprint arXiv:2401.08742*, 2024.
- [40] Yuyang Yin, Dejia Xu, Zhangyang Wang, Yao Zhao, and Yunchao Wei. 4dgen: Grounded 4d content generation with spatial-temporal consistency. *arXiv preprint arXiv:2312.17225*, 2023.
- [41] Yuan Liu, Cheng Lin, Zijiao Zeng, Xiaoxiao Long, Lingjie Liu, Taku Komura, and Wenping Wang. Syncdreamer: Generating multiview-consistent images from a single-view image. *arXiv preprint arXiv:2309.03453*, 2023.
- [42] Guangcong Wang, Peng Wang, Zhaoxi Chen, Wenping Wang, Chen Change Loy, and Ziwei Liu. Perf: Panoramic neural radiance field from a single panorama. *arXiv preprint arXiv:2310.16831*, 2023.
- [43] Huajian Huang, Yingshu Chen, Tianjian Zhang, and Sai-Kit Yeung. 360roam: Real-time indoor roaming using geometry-aware 360° radiance fields. *arXiv preprint arXiv:2208.02705*, 2022.
- [44] Kai Gu, Thomas Maugey, Sebastian Knorr, and Christine Guillemot. Omni-nerf: neural radiance field from 360 image captures. In *2022 IEEE International Conference on Multimedia and Expo (ICME)*, pages 1–6. IEEE, 2022.
- [45] Pulkit Gera, Mohammad Reza Karimi Dastjerdi, Charles Renaud, PJ Narayanan, and Jean-François Lalonde. Casual indoor hdr radiance capture from omnidirectional images. *arXiv preprint arXiv:2208.07903*, 2022.
- [46] Jiayang Bai, Letian Huang, Jie Guo, Wen Gong, Yuanqi Li, and Yanwen Guo. 360-gs: Layout-guided panoramic gaussian splatting for indoor roaming. *arXiv preprint arXiv:2402.00763*, 2024.
- [47] Zhen Xu, Sida Peng, Haotong Lin, Guangzhao He, Jiaming Sun, Yujun Shen, Hujun Bao, and Xiaowei Zhou. 4k4d: Real-time 4d view synthesis at 4k resolution. In *CVPR*, 2024.
- [48] Robin Rombach, Andreas Blattmann, Dominik Lorenz, Patrick Esser, and Björn Ommer. High-resolution image synthesis with latent diffusion models, 2021.
- [49] Yuwei Guo, Ceyuan Yang, Anyi Rao, Yaohui Wang, Yu Qiao, Dahua Lin, and Bo Dai. Animate-diff: Animate your personalized text-to-image diffusion models without specific tuning. *arXiv preprint arXiv:2307.04725*, 2023.
- [50] Zuozhuo Dai, Zhenghao Zhang, Yao Yao, Bingxue Qiu, Siyu Zhu, Long Qin, and Weizhi Wang. Animateanything: Fine-grained open domain image animation with motion guidance, 2023.
- [51] Jie An, Songyang Zhang, Harry Yang, Sonal Gupta, Jia-Bin Huang, Jiebo Luo, and Xi Yin. Latent-shift: Latent diffusion with temporal shift for efficient text-to-video generation. *arXiv preprint arXiv:2304.08477*, 2023.
- [52] Jonathan Ho, Ajay Jain, and Pieter Abbeel. Denoising diffusion probabilistic models. *Advances in neural information processing systems*, 33:6840–6851, 2020.
- [53] Omer Bar-Tal, Lior Yariv, Yaron Lipman, and Tali Dekel. Multidiffusion: Fusing diffusion paths for controlled image generation. *arXiv preprint arXiv:2302.08113*, 2023.
- [54] Andreas Lugmayr, Martin Danelljan, Andres Romero, Fisher Yu, Radu Timofte, and Luc Van Gool. Repaint: Inpainting using denoising diffusion probabilistic models. In *Proceedings of the IEEE/CVF conference on computer vision and pattern recognition*, pages 11461–11471, 2022.
- [55] René Ranftl, Alexey Bochkovskiy, and Vladlen Koltun. Vision transformers for dense prediction. In *Proceedings of the IEEE/CVF international conference on computer vision*, pages 12179–12188, 2021.
- [56] Maxime Oquab, Timothée Darcet, Théo Moutakanni, Huy Vo, Marc Szafraniec, Vasil Khalidov, Pierre Fernandez, Daniel Haziza, Francisco Massa, Alaaeldin El-Nouby, et al. Dinov2: Learning robust visual features without supervision. *arXiv preprint arXiv:2304.07193*, 2023.

- [57] Mengyang Feng, Jinlin Liu, Miaomiao Cui, and Xuansong Xie. Diffusion360: Seamless 360 degree panoramic image generation based on diffusion models. *arXiv preprint arXiv:2311.13141*, 2023.
- [58] Bangbang Yang, Wenqi Dong, Lin Ma, Wenbo Hu, Xiao Liu, Zhaopeng Cui, and Yuewen Ma. Dreamspace: Dreaming your room space with text-driven panoramic texture propagation. *arXiv e-prints*, pages arXiv–2310, 2023.
- [59] Tianhao Wu, Chuanxia Zheng, and Tat-Jen Cham. Panodiffusion: 360-degree panorama outpainting via diffusion. In *The Twelfth International Conference on Learning Representations*, 2023.
- [60] Reiner Birkel, Diana Wofk, and Matthias Müller. Midas v3.1 – a model zoo for robust monocular relative depth estimation. *arXiv preprint arXiv:2307.14460*, 2023.
- [61] Guanjun Wu, Taoran Yi, Jiemin Fang, Lingxi Xie, Xiaopeng Zhang, Wei Wei, Wenyu Liu, Qi Tian, and Xingang Wang. 4d gaussian splatting for real-time dynamic scene rendering. *arXiv preprint arXiv:2310.08528*, 2023.
- [62] Yuyang Zhao, Zhiwen Yan, Enze Xie, Lanqing Hong, Zhenguo Li, and Gim Hee Lee. Animate124: Animating one image to 4d dynamic scene. *arXiv preprint arXiv:2311.14603*, 2023.
- [63] Xingyi Li, Zhiguo Cao, Huiqiang Sun, Jianming Zhang, Ke Xian, and Guosheng Lin. 3d cinematography from a single image. In *Proceedings of the IEEE/CVF Conference on Computer Vision and Pattern Recognition (CVPR)*, pages 4595–4605, June 2023.